Corrosion properties of plasma-sprayed Al_2O_3-TiO_2 coatings on Ti metal

YO-SEUNG SONG, IN-GYU LEE, SHIN NAM HONG
Department of Materials Engineering, Hankuk Aviation University, Koyang 412-791, South Korea

BAE-YEON KIM
Department of Advanced Materials Engineering, University of Incheon, Incheon 402-749, South Korea

KOO HYUN LEE
Department of Surface Engineering, Korea Institute of Machinery and Materials, Changwon 641-010, South Korea

DEUK YONG LEE*
Department of Materials Engineering, Daelim College of Technolgy, Anyang 431-715, South Korea
E-mail: dylee@daelim.ac.kr

Published online: 17 February 2006

Three different oxides of CrO_2-TiO_2, Al_2O_3 and Al_2O_3-TiO_2 were plasma-sprayed on Ti substrate to evaluate the crystal structure and the corrosion properties of the coatings. No phase change of the coatings after corrosion test in 0.5 M H_2SO_4 solution at 25°C was found regardless of the presence of the NiCoCrAlY bond layer. Electrochemical measurements and SEM results revealed that the single coatings without the bond layer were always effective against corrosion resistance due to lower current density within the passive region. Pitting corrosion of the surface was observed for the Al_2O_3 coating. It can be concluded that the Al_2O_3-TiO_2 coating without the bond layer may be the best oxide among the oxides investigated due to low porosity (5.4%), smooth surface roughness (4.5 μm), low current density (6.3 $\times$ 10^{-8} A/cm^2) in the passive region, low corrosion potential (E_{corr}, –0.55 V) and no pitting corrosion.

1. Introduction

Ti metals have been widely used as the electrode of anticorrosion applications such as bridges, underground pipelines, cables, gas and oil tanks, structural fixtures and ships, because of their excellent electrochemical properties and corrosion resistance [1–4]. Mixed oxides on Ti metal used as anode provide remarkable corrosion resistance to increase in durability and efficiency of the components [2–4]. Our previous studies revealed that the plasma sprayed TiO_2 buffer layer between Ti substrate and sol-gel derived IrO_2-RuO_2 film was effective on improving corrosion resistance of Ti/TiO_2/IrO_2-RuO_2 anode and the addition of organic vehicle (ethyl cellulose) of an industrial infrastructure. Also, it must work under manual control for large scale operations.

Although plasma-sprayed coatings, prepared by adjusting the powder weight ratios, possess relatively high porosity and fine voids introduced by incomplete intersplat contact [8–10], the promise of plasma spraying for industrial processes (corrosion-resistance coatings on the large-scale metal structure) is very attractive due to the simplicity of the process [8, 9]. Also, the reduction in porosity can be achieved by coatings of functionally graded materials (FGMs) [10]. FGM is a gradual change in composition and microstructure of the bond-coat alloy and the top-coat oxides. Intermediate NiCoCrAlY bond

*Author to whom all correspondence should be addressed.
0022-2461
DOI: 10.1007/s10853-006-4506-6

TABLE I Plasma spray process conditions

Process variable	CrO_2-TiO_2	Al_2O_3	Al_2O_3-TiO_2	NiCoCrAlY
Primary argon gas flow rate	70 cm^3	150 cm^3	100 cm^3	150 cm^3
Secondary hydrogen gas flow rate	15 cm^3	10 cm^3	15 cm^3	15 cm^3
Powder feed rate	76 g min^{-1}	23 g min^{-1}	23 g min^{-1}	60 g min^{-1}
Gun power supply	500 V, 75 A	500 V, 75 A	500 V, 75 A	500 V, 75 A
Substrate spray distance	65 mm	65 mm	65 mm	65 mm

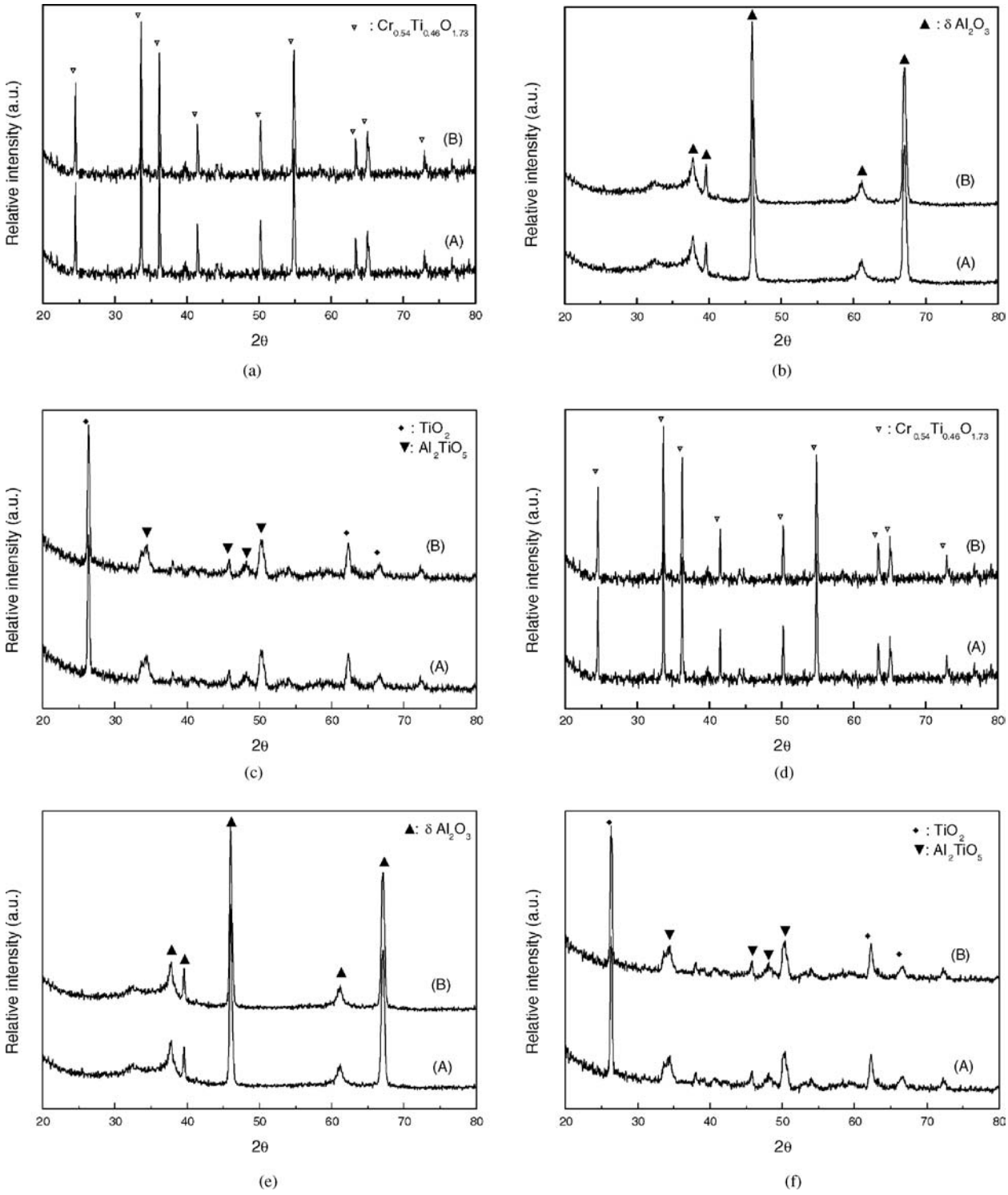

Figure 1 XRD patterns of the as-sprayed coatings (A) before and (B) after the corrosion test in 0.5 M H_2SO_4 solution at 25°C. The coatings are (a) CrO_2-TiO_2, (b) Al2O_3, (c) Al_2O_3-TiO_2, (d) NiCoCrAlY+CrO_2-TiO_2, (e) NiCoCrAlY+Al_2O_3 and (f) NiCoCrAlY+Al_2O_3-TiO_2. No phase change is observed.

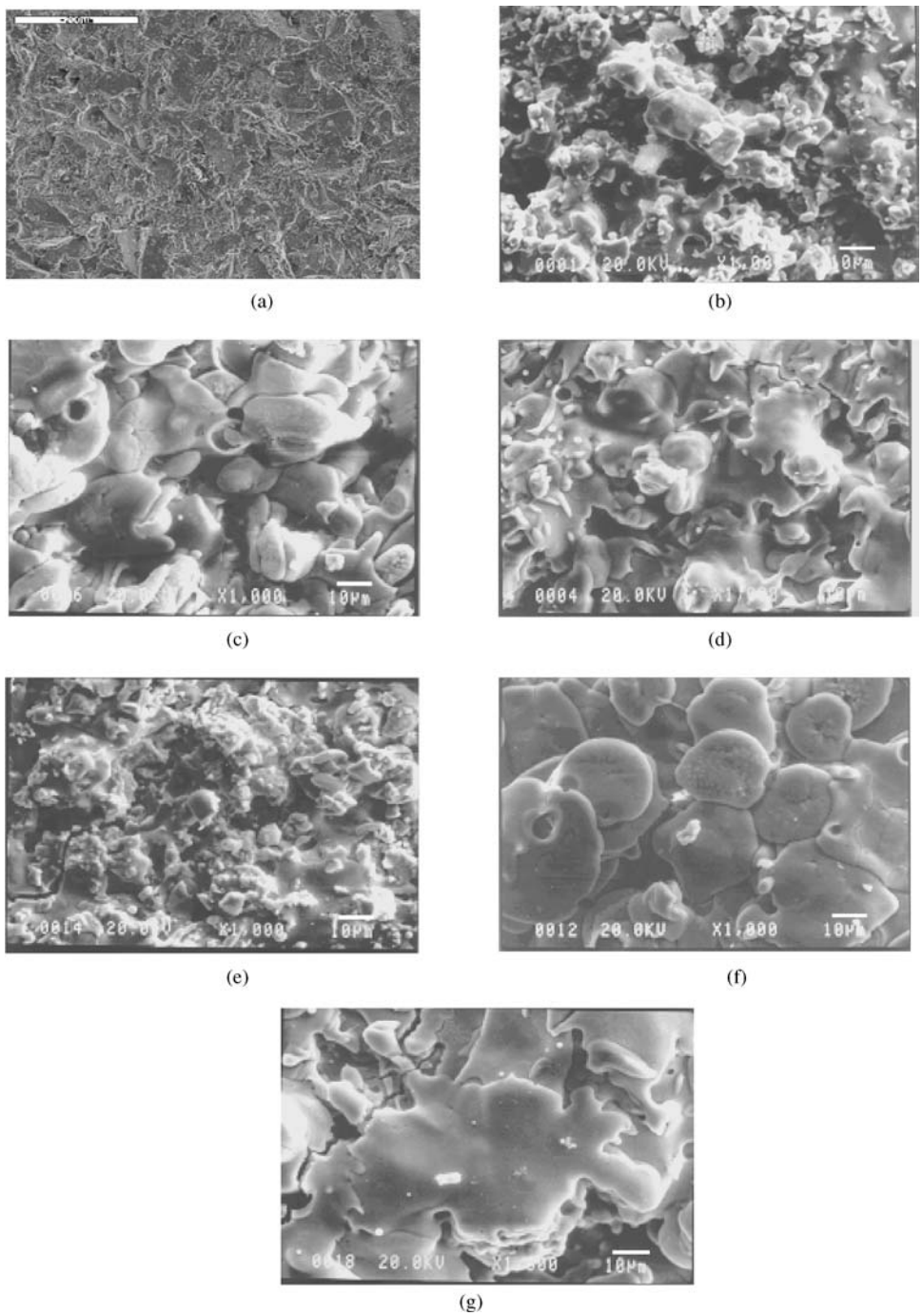

Figure 2 SEM micrographs of (a) the Ti substrate and the as-sprayed coatings: (b) CrO_2-TiO_2; (c) Al_2O_3; (d) Al_2O_3-TiO_2; (e) NiCoCrAlY+CrO_2-TiO_2; (f) NiCoCrAlY+Al_2O_3; (g) NiCoCrAlY+Al_2O_3-TiO_2.

coating is employed to alleviate thermal mismatch between top-coat oxides and Ti substrate. In the present study, three different top-coat oxides of CrO_2-TiO_2, Al_2O_3 and Al_2O_3-TiO_2, were plasma-sprayed on Ti substrate with or without the NiCoCrAlY bond alloy. Corrosion properties of the plasma-sprayed coatings were then evaluated by using X-ray diffraction (XRD) and scanning electron microscope (SEM).

2. Experimental procedure

Ti substrates with dimensions of $50 \times 50 \times 1$ mm^3 (plate type) and $20(\phi) \times 150$ mm^2 (bar type) were grit blasted using 40 mesh alumina and then surface treated using ultrasonic cleaner using distilled water, followed by heat treatment at 100∼120°C to remove the moisture. The CrO_2-TiO_2, Al_2O_3, Al_2O_3-TiO_2 and NiCoCrAlY powders were purchased from a vendor (Metco, USA) and

used without treatment. A 40 kW plasma spray system (MBN, Metco, USA) [10] was used and the plasma spray conditions were listed in Table I. Various oxides with or without the NiCoCrAlY buffer layer (200 μm) were sprayed on Ti substrate. The final thickness of the coatings was 150 μm and 350 μm, respectively.

The porosity of the coatings was determined by measuring the pore and the coating mass via image analysis technique (ASTM C1039-85) on optical micrographs [10, 11]. X-ray diffraction (XRD-3000, Rich Seifert & Co., Germany) was performed on the coatings using a Cu K_α target at a scanning rate of 0.05°/sec in the range of 20° to 80° to determine the existing phases. The microstructure and the surface roughness of the coatings were characterized by a scanning electron microscope (SEM, S-2400, Hitachi, Japan) and a Form Talysurf (Talyor Hobson, UK), respectively.

Electrochemical measurements of the specimens was conducted in 0.5 M H_2SO_4 solution at 25°C and 1500 mV (SCE) with a sweep rate of 167 mV/sec according to a potentiodynamic polarization test [5]. The potential was measured by the potentiostat in the range of –2 to +4 V.

3. Results and discussion

XRD results of the coatings, before and after the corrosion test in 0.5 M H_2SO_4 solution at 25°C, are shown in Fig. 1. No phase change was observed for all coatings regardless of the existence of the NiCoCrAlY bond layer, suggesting that the phase of the ceramic coatings is independent of the corrosion properties. McPherson [8] argued that the formation of metastable crystalline phases directly from the liquid is inevitable due to rapid cooling rate during plasma spraying [8]. Metastable δ-Al_2O_3 (Figs. 2b and e) phase rather than α-Al_2O_3, the only stable equilibrium phase, was observed experimentally for the plasma sprayed alumina onto a cooled Ti substrate. This is likely due to low nucleation energy barrier of δ-Al_2O_3 as a result of the rapid solidification during deposition [8, 12].

TABLE II Porosity and surface roughness of the as-sprayed coatings

Coatings	Porosity (%)	Surface roughness (μm)
Ti substrate	-	36.3
CrO_2-TiO_2	12.3	6.0
Al_2O_3	13.3	5.6
Al_2O_3-TiO_2	5.4	4.5
NiCoCrAlY	11.2	16.5
NiCoCrAlY + CrO_2-TiO_2	17.1	9.6
NiCoCrAlY + Al_2O_3	16.7	11.8
NiCoCrAlY + Al_2O_3-TiO_2	6.2	12.2

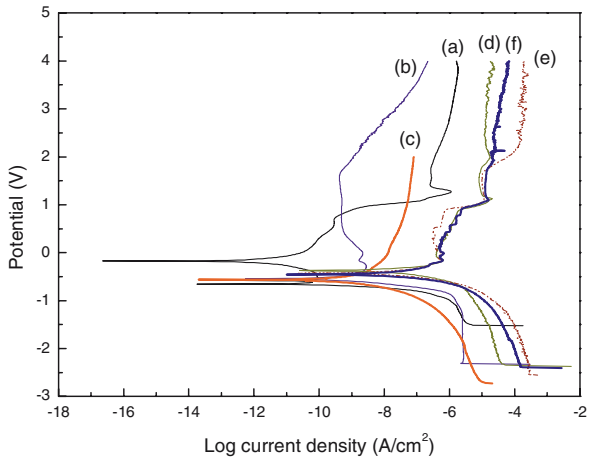

Figure 4 Polarization curves of the as-sprayed coatings containing (a) CrO_2-TiO_2, (b) Al_2O_3, (c) Al_2O_3-TiO_2, (d) NiCoCrAlY+CrO_2-TiO_2, (e) NiCoCrAlY+Al_2O_3 and (f) NiCoCrAlY+Al_2O_3-TiO_2 in 0.5 M H_2SO_4 solution at 25°C.

The porosity and surface roughness of surface-treated Ti substrate and as-sprayed coatings are summarized in Table II. The Ti substrate and the NiCoCrAlY buffer layer showed the highest roughness of 36.3 μm and 16.5 μm, respectively. The surface condition of the NiCoCrAlY buffer layer may be highly influenced by the surface roughness of the polished Ti substrate. The porosity and surface roughness of the top-coatings without the

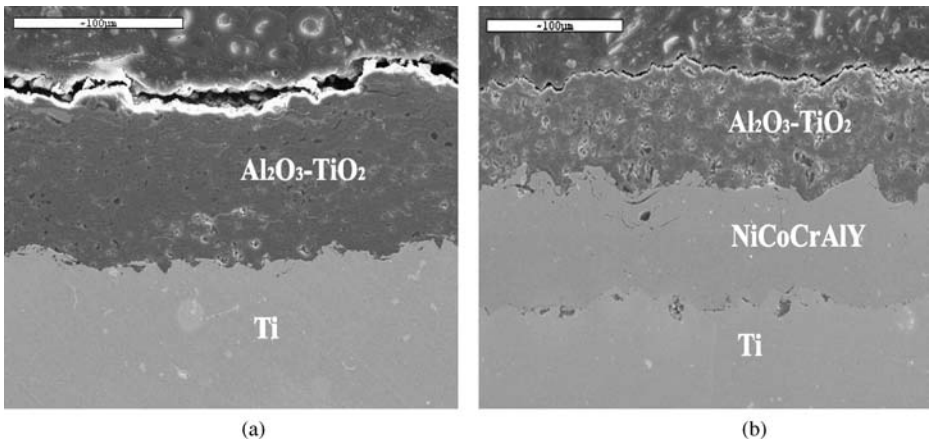

Figure 3 SEM micrographs of the cross-section of (a) Al_2O_3-TiO_2 and (b) NiCoCrAlY+Al_2O_3-TiO_2 coatings. Note that white and gray colored regions indicate TiO_2 and NiCoCrAlY, respectively.

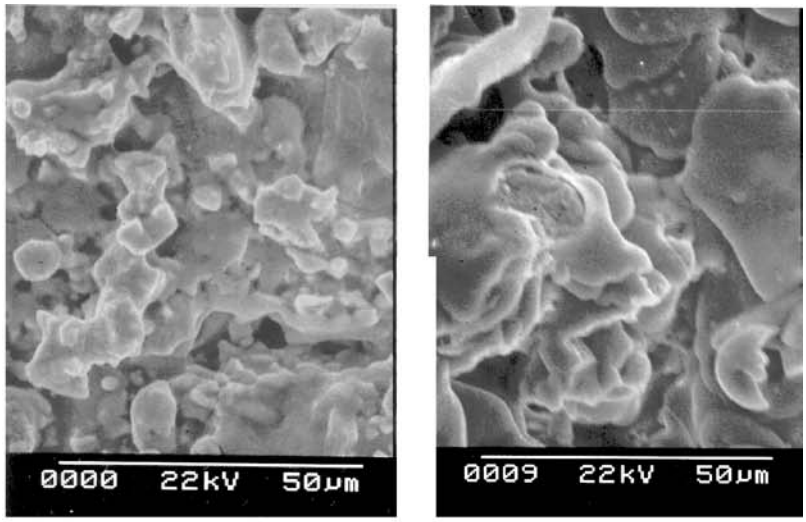

(a) (b)

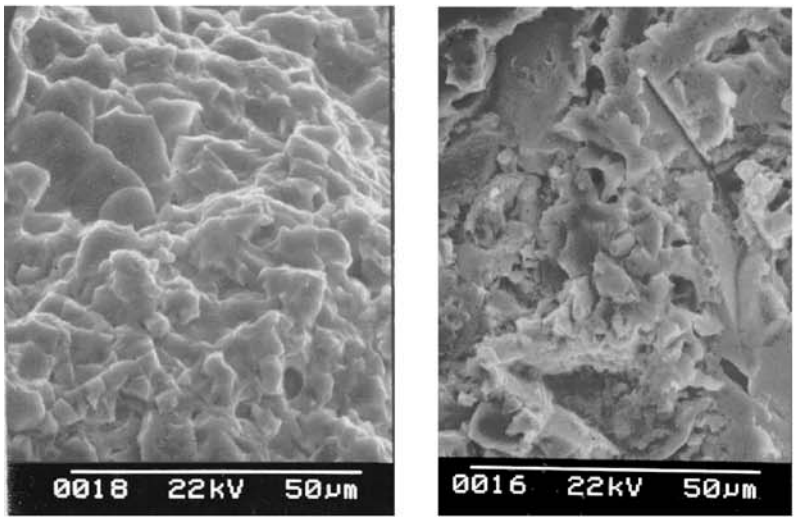

(c) (d)

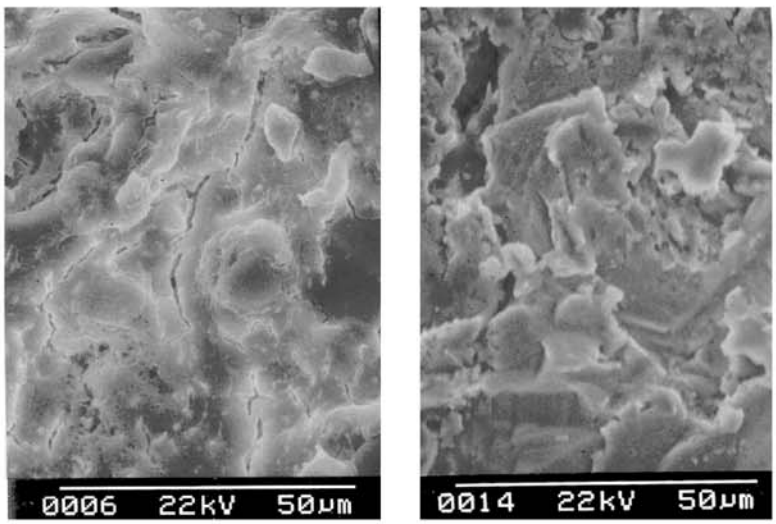

(e) (f)

Figure 5 SEM micrographs of the coatings corrosion-tested in 0.5 M H_2SO_4 solution at 25°C: (a) CrO_2-TiO_2; (b) Al_2O_3; (c) Al_2O_3-TiO_2; (d) NiCoCrAlY+CrO_2-TiO_2; (e) NiCoCrAlY+Al_2O_3; (f) NiCoCrAlY+ Al_2O_3-TiO_2.

NiCoCrAlY bond layer were superior to those of the coatings having the buffer layer. It is conceivable that higher roughness and porosity of NiCoCrAlY bond layer, as listed in Table II, may be deleterious to corrosion resistance of the successive top-coat layer, resulting in the increase in porosity and roughness of the top-coat oxide. It has been documented [8] that the porosity of the as-sprayed coatings is generally in the range of a few percent to about 20% and pores are distributed bimodally with coarse pores in the size range of 3 to 15 μm and fine pores around 0.1 μm. Cooling rate of the plasma spraying is so rapid that spreading and break up of the molten droplet is interrupted by solidification, resulting in splat quenched material. Li *et al*. [13] reported that molten or semi-molten droplets impinge on substrate and rapidly solidify into thin splats during spraying process. The coating is built up by successive impingement and interbonding of layered splats, implying that the coating may be a composite of rapidly solidified lamellae having radial growth of columnar crystal due to radial heat flow in towards the center of splat [13]. Coarse and fine pores are associated with defects in the structure due to incomplete filling of interstices between previously deposited splats and inherent defects of coatings due to rapid solidification, respectively [8]. The presence of pores and higher surface roughness may be responsible for microcracks and specific surface area, which are detrimental to mechanical, corrosion and wear properties of the coatings [2–5, 10].

SEM results of surface of the as-sprayed coatings revealed that multilayered splat morphologies consisting of irregular shaped splats and craters and pores within and between the lamellae were observed among the coatings investigated, which is directly related to the interaction between the splat formation and substrate melting and resolidification [13]. Fine spherical shaped pores within lamellae produced by rapid solidification and coarse irregular shaped pores along the lamellae introduced by incomplete filling of interstices between the splats are visible in Fig. 2. A relatively dense, smooth and compact coating was observed for the coatings containing Al_2O_3-TiO_2 and Al_2O_3 oxides as compared to those containing CrO_2-TiO_2, as can be seen in Fig. 2. SEM micrographs of cross-sections of the as-plasma sprayed coatings are depicted in Fig. 3. A compact, dense and uniform microstructure was found for the Al_2O_3-TiO_2 coatings, however, pores were visible for the Al_2O_3-TiO_2 coating containing the NiCoCrAlY bond layer.

It is noted that corrosion resistance may be counteracted by the presence of the greater porosity and roughness [8, 10, 13]. For the comparison of corrosion properties of the as-sprayed coatings on Ti substrate, the current density was measured by the potentiodynamic polarization test in 0.5 M H_2SO_4 solution. Polarization curves measured in 0.5 M H_2SO_4 solution at 25°C are shown in Fig. 4. The polarization curves show approximately equivalent characteristics except for the active and the passive peaks. All the coatings exhibit no pitting corrosion at potentials less than 4.0 V except the Al_2O_3 coating (about 1.7 V). The CrO_2-TiO_2 coating (Fig. 4a) showed double peaks in the polarization curve at the corrosion potentials (E_{corr}) of –0.65 V and –0.16 V probably due to the synergic combination of higher porosity and surface roughness. The corrosion potential rose from –0.65 V (Fig. 4a) for the CrO_2-TiO_2 coating to –0.39 V (Fig. 4d) for the NiCoCrAlY + CrO_2 – TiO_2 coating, indicating the spontaneous formation of protective passive layer for all the specimens investigated. Lower current density within the passive region was observed for the coatings in the order of Al_2O_3 < Al_2O_3 – TiO_2 < CrO_2 – TiO_2 < NiCoCrAlY + Al_2O_3 – TiO_2 < NiCoCrAlY + CrO_2 – TiO_2 ≈ NiCoCrAlY + Al_2O_3, implying that the single coatings without the NiCoCrAlY bond layer were always effective against corrosion resistance. Although the Al_2O_3 coating has the lowest current density (5×10^{-10} A/cm^2), the pitting potential was observed at about 1.7 V. Therefore, it can be concluded that the Al_2O_3-TiO_2 coating is the best oxide among the coatings investigated due to low current density (6.3×10^{-8} A/cm^2) in the passive region, low E_{corr} (–0.55 V) and no pitting corrosion at potentials less than 4.0 V. It is believed that Al_2O_3 showing a high chemical resistance may contribute to improve corrosion resistances and TiO_2 may enhance microstructure of the coating as well as interface properties between the coating and Ti substrate.

SEM micrographs of the coatings after polarization test are shown in Fig. 5. Localized corrosion (pitting corrosion) of the surface is observed for the Al_2O_3 coating as shown in Fig. 5d, which is in good agreement with the observation of the electrochemical measurements (Fig. 4b). The corrosion occurred extensively from the outer surface down to the matrix. Fig. 5 indicated that the plasma-sprayed coatings (Figs. 5d, e, f) on Ti substrate containing the NiCoCrAlY bond layer were severely corroded, which is not adequate for anticorrosion application due to high current density. A highly densified and compact microstructure was observed only for the plasma-sprayed Al_2O_3-TiO_2 coating (Figs. 2d, 3a and 5c), representing that Al_2O_3-TiO_2 oxide is highly effective on improving corrosion properties and surface microstructure of Ti substrate.

4. Conclusions

Three different oxides of CrO_2-TiO_2, Al_2O_3 and Al_2O_3-TiO_2 were plasma-sprayed on Ti substrate and the microstructure and the corrosion properties of the coatings were evaluated. As a buffer layer, NiCoCrAlY alloy was used. No phase change of the coatings tested in 0.5 M H_2SO_4 solution at 25°C was found regardless of the presence of the NiCoCrAlY bond layer, suggesting that the phase of the ceramic coatings was insignificant for corrosion properties. From the electrochemical measurements and SEM results, it suggested that the Al_2O_3-TiO_2 coating without the bond layer is the best oxide among the coatings investigated due to low

porosity (5.4%), smooth surface roughness (4.5 μm), low current density (6.3×10^{-8} A/cm^2) in the passive region, low E_{corr} (–0.55 V) and no pitting corrosion, implying that corrosion properties of the coatings were governed by porosity and surface roughness. Also, Al_2O_3-TiO_2 oxide can be applicable as plasma spraying coating materials in the large scale structures for the corrosion protection of structures such as underground pipelines and ships.

Acknowledgments

This work was supported by the Hankuk Aviation University Research Grant provided in the year of 2005.

References

1. C. ANGELINETTA, S. TRASATTI, LJ. D. ATANASOSKA, Z. S. MINEVSKI and R. T. ATANSOSKI, *Mater. Chem. Phys.* **22** (1989) 231.
2. Y. SONG, D. Y. LEE and B. KIM, *Mater. Lett.* **58** (2004) 817.
3. K. CHAE, H. CHOI, J. AHN, Y. SONG and D. Y. LEE, *Mater. Lett.* **55** (2002) 211.
4. *Idem. J. Mater. Sci.* **37** (2002) 3515.
5. K. NAM, K. LEE, S. KWON, D. Y. LEE and Y. SONG, *Mater. Lett.* **58** (2004) 3540.
6. Y. SONG, Y. NAM, K. LEE and D. Y. LEE, *Mater. Sci. Forum* **449-452** (2004) 465.
7. Y. CHOI, S. KIM, Y. SONG and D. Y. LEE, *J. Mater. Sci.* **39** (2004) 5695.
8. R. MCPHERSON, *Surf. Coat. Technol.* **39/40** (1989) 173.
9. YU. I. EVDOKIMENKO, V. M. KISEL, V. KH. KADYROV, A. A. KOROL and O. I. GET'MAN, *Powder Metallurgy Metal Ceram.* **40** (2001) 121.
10. Y. SONG, I. LEE, D. Y. LEE, D. KIM, S. KIM and K. LEE, *Mater. Sci. & Eng.* **A 332** (2002) 129.
11. K. J. KURZYDLOWSKI and B. RALPH, The Quantitative Description of the Microstructure of Materials (CRC Press, Florida, 1995) p. 356.
12. P. S. SANTOS, H. S. SANTOS and S. P. TOLEDO, *Mater. Res.* **3** (2000) 104.
13. L. LI, X. Y. WANG, G. WEI, A. VAIDYA, H. ZHANG and S. SAMPATH, *Thin Solid Films* **468** (2004) 113.

Received 12 October 2004
and accepted 17 June 2005